Journal of Alloys and Compounds 615 (2014) S85–S89

Contents lists available at ScienceDirect

Journal of Alloys and Compounds

journal homepage: www.elsevier.com/locate/jalcom

Influence of thermal treatments and plastic deformation on the atomic mobility in $Zr_{50.7}Cu_{28}Ni_9Al_{12.3}$ bulk metallic glass

J.C. Qiao, J.M. Pelletier *

Université de Lyon, CNRS, France
INSA-Lyon, MATEIS, UMR5510, F-69621 Villeurbanne, France

ARTICLE INFO

Article history:
Available online 1 December 2013

Keywords:
Bulk metallic glass
Atomic mobility
Physical aging
Plastic deformation
Physical description

ABSTRACT

The atomic mobility in $Zr_{50.7}Cu_{28}Ni_9Al_{12.3}$ bulk metallic glass has been evaluated as a function of temperature and the influence of different treatments (thermal annealing, plastic deformation) has been investigated using mechanical spectroscopy and nanoindentation technique. In particular the loss factor has been measured. This parameter is connected to the energy loss during the application of a periodic stress and therefore is sensitive to atomic movements. Master curves can be obtained, confirming the validity of the time–temperature superposition principle. The atomic mobility is reduced during physical aging (also called structural relaxation) but increased after a plastic deformation (a rejuvenation of the material is then induced). In the framework of the nanoindentation tests and mechanical spectroscopy, the concentration of "defects" in metallic glasses increases by deformation (i.e. cold-rolling) while decreases after structural relaxation and crystallization. These results are discussed using the concept of quasi-point defects, which assist the atomic movements.

1. Introduction

One of the most intriguing issues in amorphous materials concerns the physical mechanisms relative to the origin of the atomic mobility. It concerns amorphous polymers, oxides glasses, organic glasses as well as bulk metallic glasses. In crystalline materials movements of atoms or molecules are promoted by vacancies, interstitials atoms, dislocations or grain boundaries. In contrast, due to the absence of long-range order, the mechanisms of diffusion in non-crystalline solids are not so clear [1,2]. Many physical concepts have been introduced. The first one is the well known concept of free volume [3–5]. Free volume theory corresponds to a global description of the materials and was initially proposed for the liquid state. However many results reported on the mechanical properties of such materials cannot be captured by this model. Therefore other analyses have been developed and the notion of defect has been proposed by various authors [6–14]. Defects are associated to fluctuations of density, entropy, energy and may be described using the concept of potential energy landscape (PEL), initially proposed by Debenedetti and Stillinger [8]. One of the most detailed theories is that proposed by Perez [6,7], initially applied in polymers [15] but also used in bulk metallic glasses [16–19]. More recent investigations have consolidated this concept, either by computer simulation or by experiments at a nanoscale [20–22]. In any case local movements are possible in weak regions with a given activation energy. Polymers and bulk metallic glasses are both amorphous materials, but with very different chemical composition and molecular architecture. Therefore, the question is to determine if the same physical model may be used or not to capture the experimental results.

The defect concentration is sensitive to any treatment performed on the material [18,23]. An annealing below the glass transition temperature can induce a structural relaxation (physical aging), while a plastic deformation can promote a phenomenon called "rejuvenation" in polymers. In bulk metallic glasses these effects are much less documented [18,24]. Indeed most of the bulk metallic glasses are very brittle at low temperature and therefore no plastic deformation is possible [1]. Fortunately, new families have been recently developed, which exhibit a pronounced plastic deformation even at room temperature. Let us mention for instance $Zr_{50.7}Cu_{28}Ni_9Al_{12.3}$ bulk metallic glass [25]. Thus comparisons between polymers and metallic materials can now be performed.

In order to investigate the atomic mobility in solids the mechanical spectroscopy (also called dynamic mechanical analysis (DMA)) is a very suited method. A periodic stress is applied and the resulting strain is recorded. The phase lag (δ) between stress and strain is directly connected to the energy loss ($\Delta W/W$) induced during the mechanical cycle by the following equation:

* Corresponding author. Address: Université de Lyon, MATEIS, UMR CNRS5510, Bat. B. Pascal, INSA-Lyon, F-69621 Villeurbanne cedex, France. Tel.: +33 4 72 43 83 18; fax: +33 4 72 43 85 28.
E-mail address: jean-marc.pelletier@insa-lyon.fr (J.M. Pelletier).

0925-8388/$ - see front matter © 2013 Elsevier B.V. All rights reserved.
http://dx.doi.org/10.1016/j.jallcom.2013.11.158

$$\tan\delta = \frac{1}{2\pi}\frac{\Delta W}{W} \quad (1)$$

Therefore the loss factor tan δ is a direct measure of the atomic mobility. The higher is the mobility, the higher is the number of dissipative phenomena and finally the higher the loss factor.

On the other hand, the nanoindentation technique is a useful means to acquire the elastic modulus for materials at a very low load [26,27]. As we discussed previously, the mechanical properties in metallic glasses depend on the heat treatment or plastic deformation. Here, one scientific issue should be explained: does it exist any correlation between the atomic mobility and mechanical properties in metallic glasses? The present paper addresses, by using mechanical spectroscopy and nanoindentation technique, the influence of thermal treatments and plastic deformation on the atomic mobility in a bulk metallic glass which exhibits a pronounced plastic deformability at room temperature.

2. Experimental method

$Zr_{50.7}Cu_{28}Ni_9Al_{12.3}$ bulk metallic glass was prepared in melting equipment in purified argon atmosphere. All the samples were re-melted several times to improve the homogeneity. Plates with a thickness of 2 mm were made from a copper-mould casting. The composition is given in Table 1 (in at.%).

Differential scanning calorimetry (DSC) experiments were performed using a standard commercial instrument (Pekin Elmer, DSC-7) under high purity dry nitrogen at a flow rate of 20 ml/min. Continuous heating was performed at 20 K/min. Then the characteristic temperatures are determined: the glass transition temperature (T_g), the temperature corresponding to the onset of the crystallization (T_x) and then the difference between these two values ($\Delta T_x = T_x - T_g$). Results are also reported in Table 1.

X-ray diffraction (XRD) experiments were conducted at room temperature to examine their amorphous feature by Cu Kα radiation produced by a commercial device (D8, Bruker AXS Gmbh, Germany). The pattern exhibits a typical broad diffraction peak without diffraction peak corresponding to a crystalline phase, suggesting that the as-cast sample is fully amorphous. Dynamic mechanical measurements were carried out in an inverted torsion mode using a mechanical spectrometer described by Etienne et al. [28]. Experiments were performed using a sinusoidal stress, either at a fixed frequency (ranging from 10^{-4} to 1 Hz) during continuous heating with a constant heating rate or at a given temperature with different frequencies. Experimental samples with the dimension of 30 mm (length) × 2 mm (width) × 1 mm (thickness) were prepared using electric discharge machining. All the experiments were performed in a high vacuum atmosphere. Strain amplitude was lower than 10^{-4}.

Thermal treatments were performed under vacuum. Bulk metallic glass was rolled repeatedly in the same direction up to the desired deformation degree at ambient temperature [18]. The deformation (cold-rolling) degree is given by [29]:

$$\varepsilon = \frac{h_0 - h}{h_0} \quad (2)$$

where h_0 is thickness before rolling and h is the thickness after rolling in the material. This plastic deformation does not induce any crystallization, as it was observed both X-ray diffraction.

The nanoindentation tests were conducted at room temperature by commercial Nano Indenter with a Berkovich diamond tip (Agilent Nano Indenter G200) through loading control mode with a constant strain rate 0.05 s^{-1}. To ensure accuracy during the experiments, prior to nanoindentation experiments, the samples were polished carefully to mirror finishing using the 1 μm diamond paste. And the fused silica was used as a reference sample for the calibration. In the current research, at least 30 indents were carried out at same condition.

Table 1
Composition and characteristic temperatures of the investigated bulk metallic glass. Thermal parameters of the bulk metallic glass was determined by DSC at a constant heating rate 20 K/min: glass transition temperature (T_g), temperature of crystallization onset (T_x) and super-cooled liquid temperature ranges (ΔT_x, $\Delta T_x = T_x - T_g$).

Composition (at.%)	T_g (K) (±2)	T_x (K) (±2)	ΔT_x (K)
$Zr_{50.7}Cu_{28}Ni_9Al_{12.3}$	718	791	73

3. Experimental results and discussion

3.1. General tends

3.1.1. Temperature-dependence at a fixed frequency

Fig. 1 shows the amorphous characteristic at various states (i.e. as-cast, after structural relaxation and cold-rolling one) was confirmed by XRD patterns and no crystalline peak was detected. Fig. 2(a) displays the dynamic mechanical behavior, i.e. the temperature dependence of the loss factor tan δ in the $Zr_{50.7}Cu_{28}Ni_9Al_{12.3}$ bulk metallic glass. Experiments were conducted at a fixed driving frequency (0.3 Hz) and a given heating rate (3 K/min). It should be noticed that three distinct temperature domains could be detected [19,30,31]. *Region* (*I*): at low temperature the material is in the amorphous state, the behavior is elastic since the loss factor is negligible. *Region* (*II*) (when the temperature surpass 650 K): a pronounce increase in the loss factor is observed. It corresponds to the supercooled liquid region, in which the atomic motion becomes much easier. *Region* (*III*) (above about 760 K): the loss factor decreases by increasing the temperature. As a result, the crystallization occurred. Similar experimental results (not shown here) have been observed in other bulk metallic glasses [19,30,31].

In the framework of the quasi-point defect (QPD) theory [6,7], the loss factor is related to the angular frequency (ω) and the temperature (T) by the following equation:

$$\ln(\tan\delta) = -\frac{U_\beta}{kT} - \chi\ln\omega + \text{constant} \quad (3)$$

where U_β is the apparent activation energy for the atomic movement, k is the Boltzmann constant, χ is a correlation factor proportional to the defect concentration. The evolution of $\ln(\tan\delta)$ *vs* $1/T$ is reported in Fig. 2(b). A straight line is observed for low temperature values (lower than about 710 K), i.e. a value close to the glass transition temperature (NB: heating rate for DMA experiment is 3 K/min, while that for DSC experiment is 20 K/min, leading to a shift towards lower temperature for DMA measurement). Explanation is as follows: when the temperature is below the glass transition temperature, the amorphous materials remain in a frozen or isoconfigurational state. Therefore, the correlated factor χ remains constant and the mechanical behavior can be described by an Arrhenius law. In contrast, when $T > T_g$, the amorphous materials shifts to a metastable thermodynamic equilibrium and the correlation factor χ increases by increasing the temperature. Thus χ becomes temperature dependence and a straight line is no longer observed.

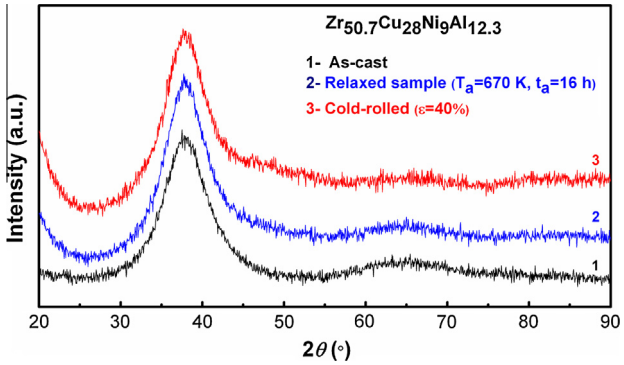

Fig. 1. XRD patterns of $Zr_{50.7}Cu_{28}Ni_9Al_{12.3}$ bulk metallic glass in different states: (1) as-cast, (2) relaxed (annealing temperature T_a = 670 K and annealing time t_a = 16 h) and (3) cold-rolled (ε = 40%).

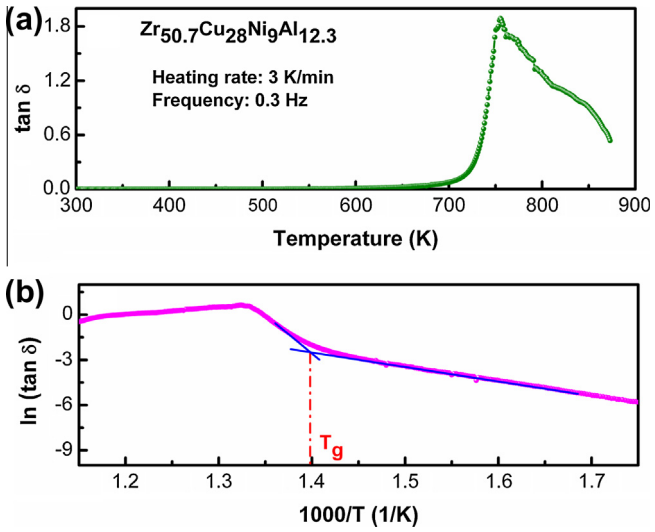

Fig. 2. (a) Evolution of the loss factor in $Zr_{50.7}Cu_{28}Ni_9Al_{12.3}$ bulk metallic glass (as-cast) as a function of temperature. (b) The plot of $\ln(\tan\delta)$ *vs* 1000/T for $Zr_{50.7}Cu_{28}Ni_9Al_{12.3}$ bulk metallic glass (as-cast). Measurement frequency is 0.3 Hz and the heating rate is 3 K/min.

3.1.2. Influence of the testing frequency

In order to well understand the influence of testing frequency on the evolution of dynamic mechanical properties of bulk metallic glass, experiments were performed at different given temperatures in a continuous frequency domain. Fig. 3(a) shows the frequency dependence of the loss factor at various temperatures (580–585–590–...725 K) for the $Zr_{50.7}Cu_{28}Ni_9Al_{12.3}$ bulk metallic glass. The investigated temperature range has been chosen so as to perform measurements only in the amorphous state. The results imply that at low temperature the loss factor increases by decreasing the frequency. On the contrary, at higher temperature a maximum peak is observed. In the framework of isothermal data at different frequencies, a master curve can be obtained by a simple horizontal shift (the reference temperature is 700 K for $Zr_{50.7}Cu_{28}Ni_9Al_{12.3}$ bulk metallic glass) (Fig. 3(b)). Therefore, the time–temperature superposition principle is valid in this alloy in the whole frequency and temperature range.

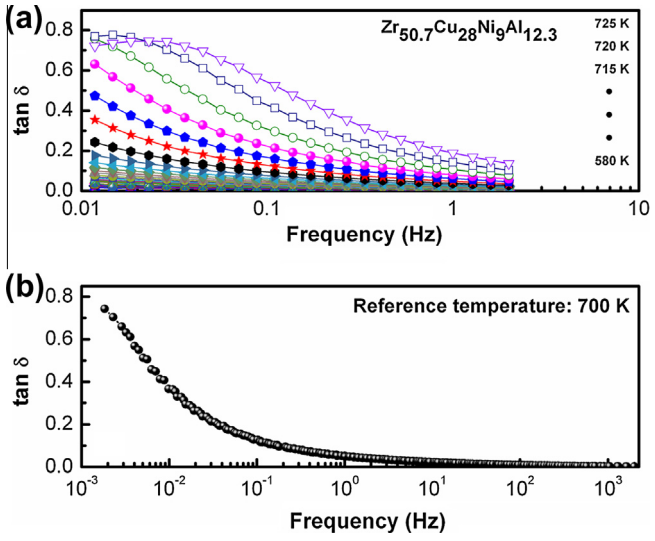

Fig. 3. (a) Dependence of the loss factor in the $Zr_{50.7}Cu_{28}Ni_9Al_{12.3}$ bulk metallic glass as a function of frequency at different temperatures (580–585–590...725 K). (b) Master curve of the loss factor in the $Zr_{50.7}Cu_{28}Ni_9Al_{12.3}$ bulk metallic glass. Reference temperature is 700 K.

3.2. Influence of a thermal annealing

The as-cast state corresponds to an out of equilibrium state. Therefore annealing can lead to an evolution towards a more stable state. A relaxed state is obtained, when annealing is carried out at fairly low temperature and/or when the annealing time t_a is not too long. A longer annealing, especially at fairly high temperature (typically above the glass transition temperature T_g) induces the crystallization process which corresponds to the most stable state. The kinetics of these evolutions depends both on alloy composition and temperature.

Fig. 4 displays for instance the evolution of the loss factor during an isothermal annealing performed at 670 K. A progressive regular decrease is observed with a progressive stabilization. At the end of the treatment, the X-ray diffraction patterns confirm that no crystalline particles were formed (see Fig. 1). Therefore this evolution corresponds only to the structural relaxation phenomenon. Theoretically time required to get a complete relaxation is infinite. However, since the equilibrium is obtained asymptotically we will consider that after 16 h nearly metastable state is achieved. This state will be considered as the reference state for the relaxed material. The loss factor decrease indicates a decrease of the atomic mobility, which can be attributed to a regular decrease in the defect concentration. The kinetics, which is accelerated when the annealing is performed at a higher temperature, may be easily described using a classical equation with a stretched exponential, as proposed for instance by Kohlrausch–Williams–Watt (KWW) [30–32].

$$\Delta = A\left\{1 - \exp\left[-(t_a/\tau)^{\beta_{KWW}}\right]\right\} \tag{4}$$

and, the similar expression in the framework of DMA experiments has been given as [30–32].

$$\tan\delta(t) - \tan\delta(t=0) = A\left\{1 - \exp[-(t_a/\tau)^{\beta}]\right\} \tag{5}$$

with $\Delta = \dfrac{\tan\delta(t) - \tan\delta(t\to\infty)}{\tan\delta(t=0) - \tan\delta(t\to\infty)}$ and A is the maximum magnitude of the relaxation.

A linear relationship is effectively observed between $\ln(\ln(-\Delta))$ and $\ln(t_a)$. Value of the Kohlrausch exponent β_{KWW} could be derived from the slope, which is around 0.494. This value is in the same range as values reported in other based amorphous alloys using DMA curves: $Cu_{46}Zr_{45}Al_7Dy_2$ ($\beta_{KWW} \sim 0.47$) [30] and $Zr_{41.2}Ti_{13.8}Cu_{12.5}Ni_{10}Be_{22.5}$ ($\beta_{KWW} \sim 0.55$) [30]. Numerous theoretical approaches have been developed to find a physical meaning to this parameter β_{KWW} [33]. But this is still an open question and the microscopic interpretation of the stretching parameter β_{KWW} varies

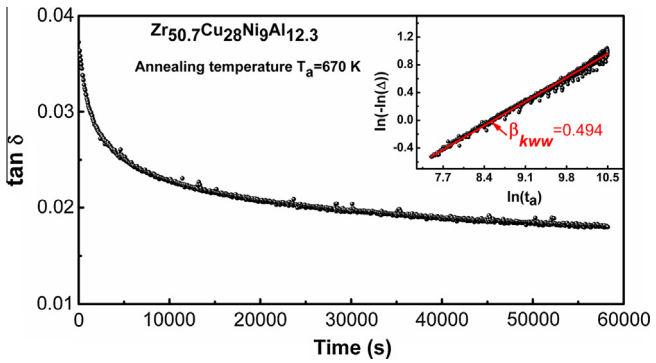

Fig. 4. Evolution of the loss factor *vs* annealing time at 670 K in $Zr_{50.7}Cu_{28}Ni_9Al_{12.3}$ bulk metallic glass. The inset is double logarithmic plot of variation of the loss factor $\tan\delta$ *vs* logarithm of the annealing time t_a.

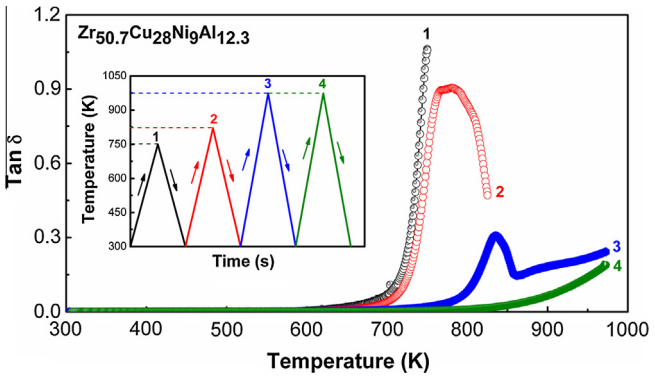

Fig. 5. Temperature dependence of the loss factor tan δ in $Zr_{50.7}Cu_{28}Ni_9Al_{12.3}$ bulk metallic glass during successive heating up to 973 K (frequency is 0.3 Hz and heating rate is 3 K/min). The inset is a scheme of the experimental process.

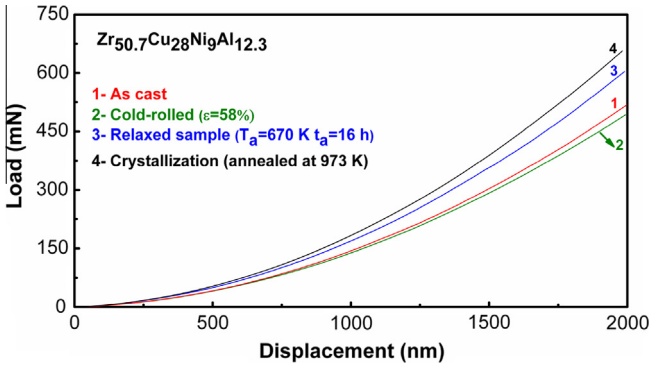

Fig. 6. Load–displacement curves with maximum indentation depth 2000 nm at a loading rate 0.05 s^{-1} in different states: (1) as-cast, (2) cold-rolled $\varepsilon = 58\%$, (3) relaxed sample (annealed at 670 K and annealing time 16 h) and (4) crystalline (heating to 973 K), respectively.

from one theory to another. Experimental values of β are in the range (0.24–1). For polymers, values extend from 0.24 (PVC) to 0.55 (polyisobutylene), for alcohols from 0.45 to 0.75, while for orientational glasses and networks values are up to 1 (for GeO_2). Bulk metallic glasses appear to be in the middle of this range. The other bulk metallic glasses [34,35] as well as amorphous polymers [36,37] has also been reported. This corresponds to a general features in all amorphous materials.

3.3. Comparison of the different states

Fig. 5 displays the evolution of the loss factor *vs* the temperature at a series of successive heating and cooling cycles during a continuous heating at 3 K/min with a driving frequency of 0.3 Hz in $Zr_{50.7}Cu_{28}Ni_9Al_{12.3}$ bulk metallic glass. It is should be noticed that the loss factor tan δ decreases progressively, which indicated that the atomic mobility decreases through the annihilation of defects.

In the view of the atomic mobility in metallic glasses, the nanoindentation tests can give another insight on the issue. Fig. 6 presents the load–displacement curves with maximum indentation depth 2000 nm at a constant loading rate 0.05 s^{-1} in different states for $Zr_{50.7}Cu_{28}Ni_9Al_{12.3}$ bulk metallic glass: as-cast, cold-rolled $\varepsilon = 58\%$, relaxed sample (annealed at 670 K and annealing time 16 h) and (4) crystalline (heating to 973 K). Clearly, compared with the as-cast state, the plastic deformation induces a lower applied load while the crystallization needs a higher applied force. To give more information on this point in a quantitative manner, the Young's modulus in different states in $Zr_{50.7}Cu_{28}Ni_9Al_{12.3}$ bulk metallic glass can be determined by the Oliver–Pharr method [38]. Vickers hardness values have been measured with a load of 0.3 kg (HV0.3). Table 2 shows the Young's modulus in $Zr_{50.7}Cu_{28}Ni_9Al_{12.3}$ bulk metallic glass at different states. On can see that the Young's modulus depends on the microstrucutral state in metallic glasses. An indicated above, a simple explanation can be given using the concept of defect introduced for instance by Perez [6,7]. The heterogeneity at a nanoscale which corresponds to fluctuations of density, entropy or elastic modulus is described as quasi-point defects. It is reasonable to conclude that the concentration of defects is decreased by the physical aging while increased by the plastic deformation. Therefore, a rejuvenation process is induced by an irreversible deformation in bulk metallic glasses, in a similar way to what is observed in polymers.

4. Summary

As in other amorphous materials the mechanical spectroscopy (or dynamic mechanical analysis (DMA)) and nanoindentation tests are very sensitive to any modification of the structural state, modifications induced by thermal annealing or plastic deformation. Since master curves can be plotted using the time–temperature superposition principle for the loss factor, a very clear representation of the atomic mobility can be obtained. The atomic mobility decreases during the structural relaxation process, but increases after a plastic deformation at room temperature. These structure modifications occur in the amorphous state, since no crystallization phenomenon is induced. These results can be easily explained using a physical model based on the concept of quasi-point defects. The heterogeneity at a nanoscale corresponds to fluctuations of density, entropy or elastic modulus is described as quasi-point defects. Their concentration tunes the atomic mobility: this concentration is decreased during the physical aging phenomena (or structural relaxation phenomenon), while the plastic deformation induces an increase in this concentration. This last phenomenon corresponds to a rejuvenation of the material, by opposition to the physical aging.

Acknowledgments

One of the authors, J.C. Qiao would like to thank the Centre National de la Recherche Scientifique (CNRS) for providing the post-doctoral financial support. We thank W.H. Wang's group (Institute of Physics, CAS) for providing the samples.

Table 2
The Young's modulus was determined using the load–displacement curves with maximum indentation depth 2000 nm at a loading rate 0.05 mN/s in different states: (1) as-cast, (2) cold-rolled $\varepsilon = 58\%$, (3) relaxed sample (annealed at 670 K and annealing time 16 h), and (4) crystalline (heating to 973 K), respectively. The Young's modulus is determined by the Oliver–Pharr method [38].

Microstructural state	Cold-rolled	As cast	Relaxed sample	Crystalline
Young's modulus (GPa)	108.1 ± 1.4	112 ± 3	139.5 ± 2.6	152.9 ± 7.4

References

[1] W.H. Wang, Prog. Mater. Sci. 57 (2012) 487.
[2] R. Richert, K. Samwer, New J. Phys. 9 (2007) 36.
[3] A.K. Doolittle, J. Appl. Phys. 22 (1951) 1471.
[4] M.H. Cohen, D. Turnbull, J. Chem. Phys. 31 (1959) 1164.
[5] D. Turnbull, M.H. Cohen, J. Chem. Phys. 34 (1964) 120.
[6] J. Perez, Polymer 29 (1988) 483.
[7] J. Perez, Solid State Ionics 39 (1990) 69.
[8] P.G. Debenedetti, F.H. Stillinger, Nature 410 (2001) 259.
[9] F.H. Stillinger, Science 267 (1995) 1935.
[10] A.S. Argon, Acta Metall. 27 (1979) 47.
[11] A.S. Argon, Acta Metall. 31 (1983) 499.
[12] T. Egami, J. Alloys Comp. 509S (2011) S82.
[13] W. Dmowski, T. Iwashita, A. Chuang, J. Almer, T. Egami, Phys. Rev. Lett. 105 (2010) 205502.
[14] T. Egami, J. Mater. Sci. 13 (1978) 2587.
[15] R. Rinaldi, R. Gaertner, L. Chazeau, G. Gauthier, Int. J. Nonlinear Mech. 46 (2011) 496.
[16] J.C. Qiao, J.M. Pelletier, Intermetallics 19 (2011) 9.
[17] J.M. Pelletier, D.V. Louzguine-Luzgin, S. Li, A. Inoue, Acta Mater. 59 (2011) 2797.
[18] J.C. Qiao, J.M. Pelletier, H.C. Kou, X. Zhou, Intermetallics 28 (2012) 128.
[19] J.C. Qiao, J.M. Pelletier, J. Appl. Phys. 112 (2012) 033518.
[20] Y.H. Liu, D. Wang, K. Nakajima, W. Zhang, A. Hirata, T. Nishi, A. Inoue, M.W. Chen, Phys. Rev. Lett. 106 (2011) 125504.
[21] M.H. Lee, J.K. Lee, K.T. Kim, J. Thomas, J. Das, U. Kühn, J. Eckert, Phys. Status Solidi RRL 3 (2009) 46.
[22] J.W. Deng, K. Du, M.L. Sui, Micron 43 (2012) 827.
[23] E. Munch, J.M. Pelletier, B. Sixou, G. Vigier, Phys. Rev. Lett. 97 (2006) 207801.
[24] J.M. Pelletier, Y. Yokoyama, A. Inoue, Mater. Trans. 48 (2007) 1359.
[25] F.F. Wu, W. Zhang, J.W. Deng, D.D. Qu, J. Shen, Mater. Sci. Eng. A 541 (2012) 199.
[26] S. Xie, E.P. George, Acta Mater. 56 (2008) 5202.
[27] Y.J. Huang, Y.L. Chiu, J. Shen, J.J.J. Chen, J.F. Sun, J. Alloys Comp. 479 (2009) 121.
[28] S. Etienne, J.Y. Cavaillé, J. Perez, R. Point, M. Salvia, Rev. Sci. Instrum. 53 (1982) 1261.
[29] P.N. Zhang, J.F. Liu, Y. Hu, Y.H. Zhou, J. Mater. Sci. 43 (2008) 7179.
[30] J.C. Qiao, J.M. Pelletier, Intermetallics 28 (2012) 40.
[31] J.C. Qiao, J.M. Pelletier, R. Casalini, J. Phys. Chem. B 117 (2013) 13658.
[32] J.M. Pelletier, J. Non-Cryst. Solids 354 (2008) 3666.
[33] S.G. Mayr, Phys. Rev. B 79 (2009) 060201.
[34] L.M. Wang, R.P. Liu, W.H. Wang, J. Chem. Phys. 128 (2008) 164503.
[35] L.M. Wang, Z.M. Chen, Y. Zhao, R.P. Liu, Y.J. Tian, J. Alloys Comp. 504S (2010) S201.
[36] A.C. Comer, A.L. Heilman, D.S. Kalika, Polymer 51 (2010) 5245.
[37] R. Casalini, A.W. Snow, C.M. Roland, Macromolecules 46 (2013) 330.
[38] W.C. Oliver, G.M. Pharr, J. Mater. Res. 7 (1992) 1564.